Size effect in circularly symmetric, annular Josephson junctions and the role of an applied magnetic field

Qianghua Wang
Physics Department, Nanjing University, Nanjing 210008, People's Republic of China

Wei Wang
Chinese Center of Advanced Science and Technology (World Laboratory) P.O. Box 8730, Beijing 100080, People's Republic of China
and Department of Physics and The Center of Nonlinear Dynamical System, Nanjing University, Nanjing 210008, People's Republic of China

Xixian Yao
Department of Physics and The Center of Nonlinear Dynamical System, Nanjing University, Nanjing 210008, People's Republic of China
(Received 31 March 1992)

The size effect in circularly symmetric, annular Josephson junctions is discussed in detail. For a junction of width W, we find that there exists a minimum inner radius $\rho_{\min}$ for resonant soliton motion within the junction, with respect to the dissipative parameter and external magnetic field, and that the applied magnetic field plays an important role in reducing the size effect ($\rho_{\min}$ decreases remarkably in the presence of a negative external magnetic field). Because of the size effect, the range of the first current step vanishes if the inner radius of the annular junction is smaller than $\rho_{\min}$. A qualitative interpretation is given for the size effect. On the basis of our results, future physical experiments are suggested.

I. INTRODUCTION

The sine-Gordon partial-differential wave equation (SGE) plays a major role in nonlinear physics. Its success in modeling a variety of nonlinear phenomena has been emphasized in the papers of Perring and Skyrme[1] and Scott.[2] Some specific applications that come to mind are the following: propagation of fluxons in Josephson junctions,[3] propagation of crystal dislocations,[4,5] elemental excitations in charge-density-wave systems,[6] and domain-wall motion in antiferromagnetic materials.[7] The SGE possesses a remarkable soliton solution (2π-kink solution), which has been fully discussed by Ablowitz *et al.* by the inverse-scattering method.[8] A system in which soliton propagation is most accessible to experimental measurement is the large-area Josephson junction, as has been well described in a book by Barone and Pagano.[9] Fluxon excitation in long or large-area Josephson junctions has been considered for application, for example, as microwave generators in high-frequency integrated circuits and data-processing systems. In Josephson junctions, the physical manifestation of a soliton is a fluxon, i.e., a quantum of magnetic flux $\Phi = h/2e$. The simplest and most direct way of measuring moving fluxons is to measure the so-called zero-field states (ZFS) in the dc I-V curve (more generally, the steplike singularity in the I-V curve if there is a small dc applied field). The first ZFS is explained as a resonant motion of a single fluxon along the junction. Higher-order steps are numbered according to the total number of fluxons and antifluxons. Their motion is, in general, governed by a perturbed SGE (in the presence of damping and dissipation), subject to boundary conditions determined by such factors as the geometry, the current distribution, the load, and the external magnetic field. To understand the behavior of the solitons in the perturbed system, several perturbation theories have been developed, based, for example, on the linear perturbation scheme,[10,11] the inverse scattering method,[12,13] and Green's-function approach.[14] Using the technique developed by McLaughlin and Scott,[14] some authors have recently analyzed the behavior of the solitons in 1D long junctions and their I-V characteristics (cf. Ref. 15). However, because of complexities of the perturbation schemes understanding of these systems is often only achieved by performing direct numerical simulations or physical experiments.

Apart from the usual configurations such as 1D long transmission line and narrow annual junctions (which is equivalent to a 1D long junction with spatial periodicity of $L = 2\pi R$), we have recently considered a wide annular junction with circular symmetry, which is geometrically equivalent to an infinite number of parallel-coupled in-line junctions and therefore is assumed to have a radiation power comparable to those of coupled in-line junctions. A circularly symmetric, annular Josephson junction is shown schematically in Fig. 1. The annular width W is equal to the difference of the outer radius ρ_o and the inner radius ρ_i of the junction, $W = (\rho_o - \rho_i)\lambda_J$. In the overlap region the superconductors are separated by a thin insulating layer; the feeding current I' flows along the Z direction, and the external field is produced by a current I'_H that flows in another conducting wire located at the center of the junction. The dimensionless dynamical equation is taken to be the modified sine-Gordon

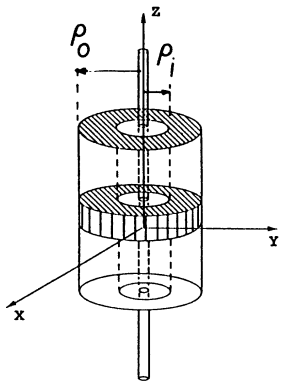

FIG. 1. Annular Josephson-junction configuration. The annular width W is equal to the difference of the outer radius ρ_o and the inner radius ρ_i of the junction, $W=(\rho_o-\rho_i)\lambda_J$. In the overlap region the superconductors are separated by a thin insulating layer; the input current I' flows along the Z direction, and the external field is produced by a current I'_H that flows in another conducting wire located at the center of the junction.

equation[16,17]

$$\phi_{\rho\rho}+\frac{1}{\rho}\phi_\rho-\phi_{tt}-\alpha\phi_t=\sin\phi \tag{1}$$

with boundary conditions

$$\phi_\rho|_{\rho=\rho_i}=I'_H/2\pi\rho_i=\kappa_i \tag{2}$$

and

$$\phi_\rho|_{\rho=\rho_o}=\frac{I'_H+I'}{2\pi\rho_o}=\kappa_o+\eta\ , \tag{3}$$

where $\kappa_o=I'_H/2\pi\rho_o$ and $\eta=I'/2\pi\rho_o$. Here, the time t is normalized by $\lambda_J/\bar{c}$, the space ρ by λ_J, and feeding current I' (I'_H as well) by $J_c\lambda_J^2$. It is understood that all quantities mentioned hereafter are dimensionless according to these normalizations. In Eq. (1), ϕ is the local phase difference of the order parameters in separated superconductors, subscripts denote partial differentiation, and $\alpha\phi_t$ represents the dissipation effect due to the tunneling of normal electrons across the barrier. In Eq. (3), I' is the feeding current. Eqs. (2) and (3) result from Ampere's law for ϕ_ρ and I' and I'_H (since ϕ_ρ represents the local magnetic field in our system). $\kappa_{i,o}$ measures the contribution of the applied magnetic field at the boundaries (κ_i and κ_o are dependent), while η measures the contribution of the feeding current to the magnetic field at the outer boundary, and the equivalent line density of feeding current along an outer circle in analogy to the definition in the case of an in-line junction. The renormalized quantities $\kappa_{i,o}$ and η are introduced and used hereafter in this paper, since they describe exactly the extent of the perturbation to the system.

The reason why we have introduced this model is that a circular junction does not support stable circularly symmetric soliton (CS soliton hereafter) motion, while an annular junction does under certain conditions, as has been confirmed by our earlier studies.[16–21] We remark that Christiansen and Olsen have investigated numerically the rotational symmetric, solitary-wave (or ring-wave) solutions to the SGE with geometric dimension $m=2,3$.[22,23] They found that an expanding ring wave reaches a maximum size, depending on the initial conditions, and then shrinks. This phenomenon was called the return effect, which does not occur in the 1D case. Their further studies showed that the interaction between the ring waves does not change their identity, and the ring waves were denoted quasisolitons (CS soliton in the present paper). However, the evolution of the CS soliton breaks down because of the reflection at the origin.[24,25] Therefore, the circular model is not feasible for physical application. In practice, the soliton return effect could still exist in annular junctions; however, it can be avoided. We have previously discussed the return effect both in the absence of dissipation[16] and in the presence of dissipation, as well as its relationship with the I-V characteristic.[18] We noted[18] that a returning CS soliton (or equivalently the bound soliton and virtual antisoliton pair, the breather) is dissipated and the final solution is a static one with the associated average voltage across the junction being zero. Mostly, the return effect can be eliminated from our model and resonant CS soliton motion can be achieved by increasing the feeding current. However, for the specific case of an annular junction [e.g., the $1/\rho$ term in Eq. (1), the boundary conditions described by Eqs. (2) and (3)], this does not always work, and so the single-CS-soliton state might not exist at all if the geometrical size is not chosen properly. As a matter of fact, for a junction with width W, there exists a minimum inner radius $\rho_i=\rho_{\min}$ of the junction, such that resonant CS soliton motion is possible only if $\rho_i>\rho_{\min}$—this is called the size effect in the present paper, as will become clear in the following discussions. Introducing a negative external magnetic field can reduce the size effect significantly, since $\rho_{\min}$ in this situation is much smaller. We assume that in the 1D case, the size effect is not so significant, especially for an overlap junction, although no detailed discussion exists on the problem in the literature.

Since the question of the existence of CS soliton states in real systems is of considerable practical interest for experimentalists, and, since no completely adequate analytic or perturbative approach is presently available to us, we propose in this work to carry out a detailed numerical study of this question, with the hope of providing a springboard for future theoretical work. We note that relevant problems have recently been addressed by several authors in other directions.[26–30] In contrast to their works, we emphasize the instability mechanism of CS solitons due to the boundary conditions and explore thereby, as a first step, the size effect numerically. Like the other authors, we limit ourselves to consideration of dynamic states involving single-CS soliton propagation. Moreover, effects of intrinsic and extrinsic noise, the angular perturbation, and geometric imperfection on the stability of the fluxon are beyond the scope of the present study. This choice is made easier because the cited noise, though often important in physical devices, can always be reduced by careful shielding of the junction from possible electromagnetic interference, by lowering the working

temperature, and by improving the fabrication processes; in addition, the angular perturbation is not considered a crucial factor in a system with circular symmetry. This latter point has been addressed by some relevant studies on CS-pulse excitations in the ϕ^4 model and sine-Gordon system[31] in which these excitations turn out to be stable against small perturbations in the absence of dissipation. Such an angular stability is inherent to the self-forming long-lived pulse excitations of large amplitude in the above framework with degenerated vacua. A natural interpretation of this result is the following: The angle-variable independence of the solutions minimizes the Hamiltonian. We believe that this stability is enhanced in the presence of dissipation in our system. The results of our computations, which corroborate this interpretation, will be presented elsewhere. Therefore, the maximum performances of the junction will be determined by the intrinsic instability of the fluxon oscillation in this work. The remainder of this paper is organized as follows: Numerical experiments are described and discussions on the size effect are given in Sec. II; and a summary is presented in Sec. III.

II. NUMERICAL EXPERIMENTS AND DISCUSSION ON THE SIZE EFFECT

A. Numerical experiments

We assume that a CS soliton solution can be taken as the zeroth-order initial solution of the modified SGE, i.e., Eq. (1):

$$\phi = 4\tan^{-1}\exp\left[\frac{\sigma[\rho - R(t)]}{(1-u^2)^{1/2}}\right], \tag{4}$$

$$\phi_t = \frac{-2\sigma u}{(1-u^2)^{1/2}}\operatorname{sech}\left[\frac{\sigma[\rho - R(t)]}{(1-u^2)^{1/2}}\right], \tag{5}$$

where $\sigma = \pm 1$ is the polarity of soliton and antisoliton, respectively. Hereafter, we will not distinguish between soliton or an antisoliton except where possible confusion might arise. The function $R(t)$ describes the center position of the fluxon, i.e., the maximum of ϕ_t.

We use an implicit finite-difference method with respect to space ρ, and the fourth-order Runge-Kutta integration with respect to time t together with the initial conditions Eqs. (4) and (5) to evaluate the evolution of discretized ϕ and ϕ_t, etc. The precision and stability of computation are carefully checked to guard against any spurious results. In our double-precision computation, the step of space $\delta\rho$ and the step of time δt, are, respectively, 0.075 and 0.05, which already provide satisfactory precision and numerical stability. The average voltage of the junction is given by

$$V = \langle \phi_t \rangle , \tag{6}$$

which is the spatio-temporal average of ϕ_t. The CS soliton motion and the relevant I-V characteristic under various conditions have been discussed in Ref. 20 both analytically and numerically; the I-V curves need not be reproduced in this paper. As has been explained in the introduction, the physical manifestation of a moving soliton (fluxon) in a Josephson junction is the steplike singularity (current step) in the I-V curves. On the other hand, a static CS soliton state does not exist in circularly symmetric sine-Gordon system, due to the effective attraction of the origin acting on the CS solitons.[18–20] Therefore, the current step is sensitive to the existence of resonant CS soliton motion in our case, and the current range of the current step serves to be a coarse measure of the stability of the CS soliton state against the perturbations.

We explore the size effect, or the minimum inner radius $\rho_{\min}$ for stable CS soliton motion in the annular junctions with $W=7.5$ and $\alpha=0.06$, in the following manner. For a fixed applied magnetic field measured by κ_i, we calculate the I-V characteristic of the junction with an inner radius ρ_i, and then another one of smaller ρ_i, using the algorithm described above. To avoid the transient effect, the computation is taken for each initial condition and feeding current until a stable final state settles down. As has been explained previously, the current range $\Delta\eta$ of the current step in the I-V curve is a measure, in some sense, of the stability of CS soliton motion against perturbations. If $\Delta\eta$ vanishes as $\rho_i \to \rho_{\min}$, we are done, and $\rho_{\min}$ is the minimum inner radius of the junctions (with respect to κ_i, W, and α) supporting CS soliton motion. Figure 2 shows the current range $\Delta\eta$ versus ρ_i, for $\kappa_i=0$ (A; squares), $\kappa_i=-0.56$ (B; circles), and $\kappa_i=0.2$ (C; triangles). It is clear from Fig. 2 that a negative (positive) applied field enhances (reduces) the stability of CS soliton motion compared with the case of zero applied field. On the other hand, the minimum inner radii for different applied fields are, $\rho_{\min}=1.55$ for $\kappa_i=-0.56$, $\rho_{\min}=5$ for $\kappa_i=0$, and $\rho_{\min}=10$ for $\kappa_i=0.2$ Therefore, the size effect can be reduced significantly by a negative applied field, which suggests possible physical experiments. Finally, as

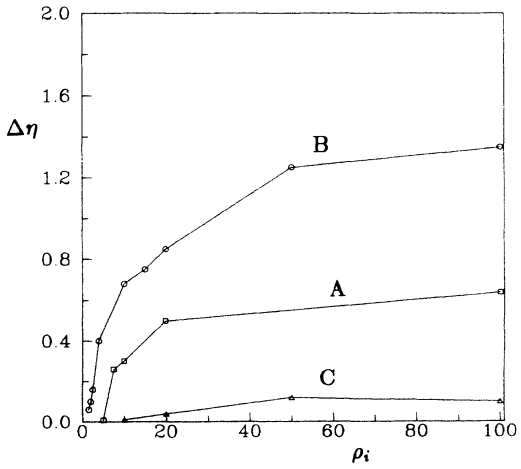

FIG. 2. The dependence of the current range $\Delta\eta$ in the first current step on the inner radius ρ_i of the junctions with $\alpha=0.06$ and $W=7.5$ and under different applied field. A (squares): $\kappa_i=0$ (zero field); B (circles): $\kappa_i=-0.56$; C (triangles): $\kappa_i=0.2$. Lines in the figure are presented as guides for the eye. All quantities are normalized and dimensionless (see the text).

$\rho_i \to \infty$, the $1/\rho$ term in Eq. (1) has a minor effect on CS soliton motion, and the current range tends naturally to that in 1D case. We believe that the size effect, besides the soliton return effect discussed elsewhere,[18] is typical in 2D and 3D SGE systems with rotational symmetry.

To understand the size effect in annular junctions, we also emphasize the important role of boundary conditions, since they are the only factors with which the feeding current can affect CS soliton motion within the junction. For a definite κ_i, we are only concerned with the external boundary condition (EBC),

$$\phi_\rho(\rho=\rho_o)=\kappa_o+\eta=\kappa_i\rho_i/(\rho_i+W)+\eta \ . \tag{7}$$

For a definite κ_i, ρ_i, and W, we explore the upper and lower limit of the EBC, with the hope of searching for the background of the state switching at the ends of the current step in the I-V curve. The current range is obtained from the spacing between the lower and upper limits of the EBC. In Fig. 3 we show the limits of the EBC versus ρ_i for $\kappa_i=0$ [Fig. 3(a)], $\kappa_i=-0.56$ [Fig. 3(b)], and $\kappa_i=0.2$ [Fig. 3(c)]. The insertions in Figs. 3(a) and 3(b) are more complete representations of the ρ_i dependence of the EBC limits with wider range of ρ_i. Lines A and B represent the upper and lower limit of the EBC, respectively, in Fig. 3. For nonpositive κ_i, from Figs. 3(a) and 3(b) we see that the lower (upper) limit of EBC, which relates to the minimum (maximum) feeding current for CS soliton motion, increases (decreases) with decreasing ρ_i, and lines A and B intersect at $\rho_i=\rho_{\min}$; on the other hand, lines A and B saturate with $\rho_i \to \infty$. However, for positive κ_i, the vertical spacing between lines A and B, or the current range of the current step, remains small for

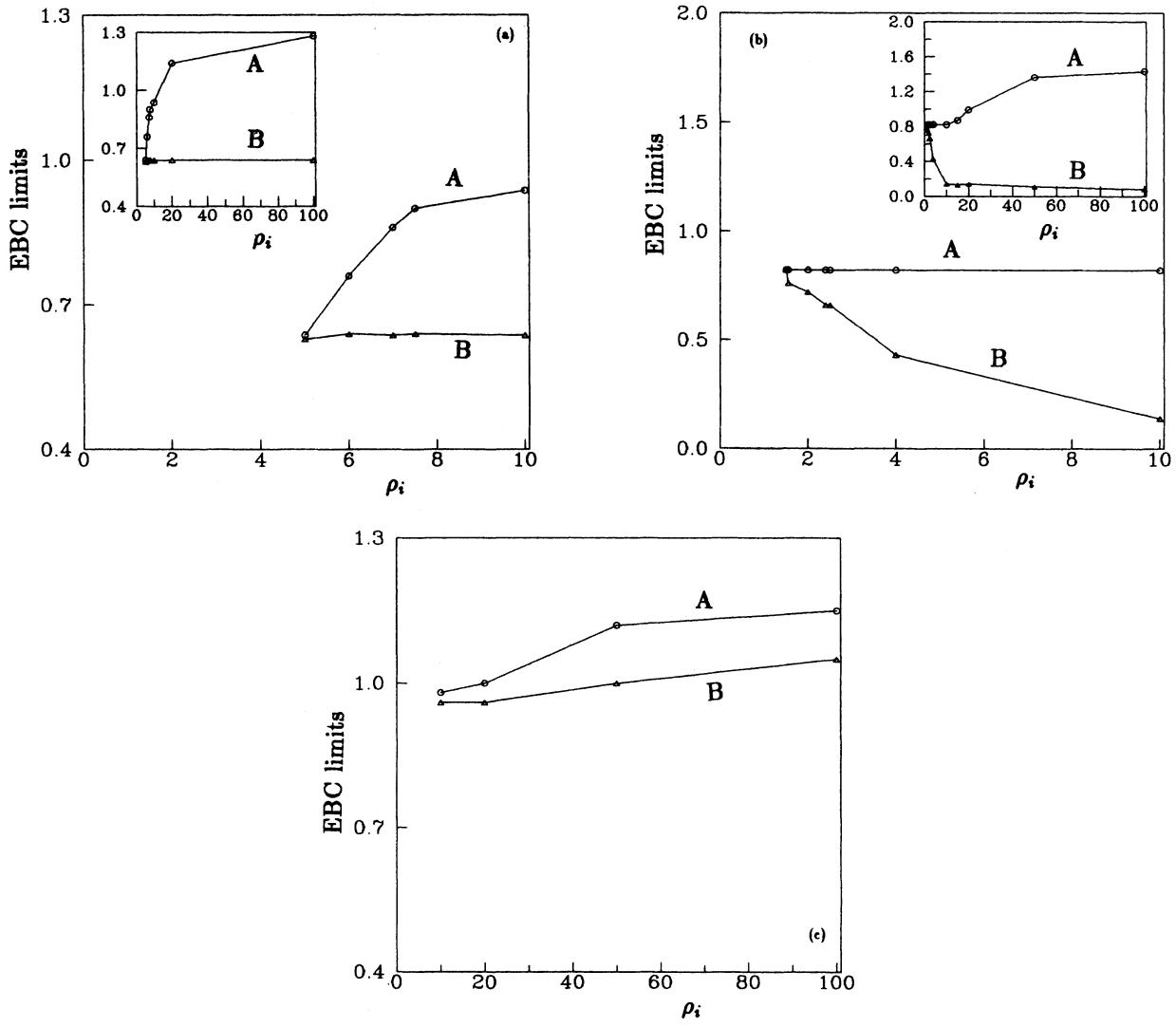

FIG. 3. (a) The dependences on the inner radius ρ_i of the upper (A) and lower (B) limits of the external boundary condition (EBC, see the text) $\phi_\rho(\rho=\rho_o)$ for CS soliton motion for junctions with $W=7.5$ and $\alpha=0.06$ and under zero applied field ($\kappa_i=0$). The insertion in the figure is a more complete representation of the relation for wider range of ρ_i. Lines in the figures are presented as guides for the eye. All quantities are normalized and dimensionless. (b) The same as Fig. 3(a) except that $\kappa_i=-0.56$. (c) The same as Fig. 3(a) except that $\kappa_i=0.2$.

large ρ_i. This is due to the special configuration and the current-injection conditions, i.e., the special boundary conditions used. Notable is the slope change of line B in Fig. 3(b) when $\rho_i \simeq 10$ (see the insertion). It will become clear in the following discussion. It is obvious that the understanding of both the lower and upper limits of the EBC is essential for analytical exploration of the size effect.

B. Discussion on the EBC limits

The lower limit of the EBC is related to the minimum feeding current, which results from such factors as the soliton return effect discussed in Ref. 18 and the dissipation due to the reflection of the soliton at the boundaries.[35,36] Since the perturbation due to the boundary condition under minimum bias is small, we can employ the perturbative treatment developed elsewhere,[18,19] provided that $\rho_i \geq 5$, so that the $1/\rho$ term in Eq. (1) can also be taken as a perturbation. For still smaller ρ_i, e.g., $2 < \rho_i < 5$, the perturbative treatment is in principle questionable; however, these results are only suggestive. A detailed discussion on this problem will be given elsewhere. Here we only outline the determination of the lower limit of the EBC here by referring to Ref. 18. The energy of the junction is defined as

$$E = \int d\rho \, 2\pi\rho [\tfrac{1}{2}(\phi_t^2 + \phi_\rho^2) + 1 - \cos\phi] \ . \tag{8}$$

The energy of a CS soliton is

$$E = 16\pi R / \sqrt{1-u^2} \ , \tag{9}$$

where R and u are the position and velocity of the CS soliton, respectively. The dynamical equation that describes CS soliton motion within the junction is

$$du/dt = -(1-u^2)/R - \alpha u (1-u^2) \ , \tag{10}$$

where du/dt is the acceleration of the CS soliton. In Ref. 18, the applied field was zero, and the dissipation due to the reflection was not taken into account. However, we would like to point out that it is straightforward to generalize the treatment in Ref. 18 to various applied fields, and to extend the treatment of reflection dissipation in 1D junctions ($\Delta H \simeq -4\pi^2\alpha$ Refs. 35 and 36) into the one used in our model. For example, the reflection dissipation will be

$$\delta E_i = 2\pi\rho_i \, \Delta H \tag{11}$$

at the inner boundary, and

$$\delta E_o = 2\pi\rho_e \, \Delta H \ , \tag{12}$$

where $\Delta H \simeq -4\pi^2\alpha$. The energy input from the boundary to the CS soliton, when it is reflected is

$$\Delta E_i = -4\pi I'_H = -8\pi^2 \rho_i \kappa_i \tag{13}$$

at the inner boundary, and

$$\Delta E_o = 4\pi (I' + I'_H) = 8\pi^2 \rho_o (\eta + \kappa_o) \tag{14}$$

at the outer boundary. (Note that $I'_H = 2\pi\rho_i\kappa_i = 2\pi\rho_o\kappa_o$). It is clear that the applied field provides no net energy input to the CS soliton during a period of back and forth motion, but $\Delta E_i > 0$ if $\kappa_i < 0$, therefore the negative applied field serves to be an energy station for the CS soliton motion, and this is essential for the CS soliton to expand with a large enough velocity to overcome the strong effective attraction of the origin (especially when ρ_i is small).[18] In other words, a negative applied field is favorable to CS soliton motion. Considering the reflection dissipation δE_i and δE_o, we have the effective energy input when the CS soliton is reflected at the inner boundary

$$\Delta E_i^{\text{eff}} = \Delta E_i + \delta E_i \ , \tag{15}$$

and the effective one at the outer boundary

$$\Delta E_o^{\text{eff}} = \Delta E_o + \delta E_o \ . \tag{16}$$

The minimum feeding current can be obtained from the minimum energy dissipated within the junction. Suppose that u_{fm} is the minimum velocity with which the CS soliton can expand to the outer boundary (in zero applied field, u_{fm} is certainly zero), and u_{im} is the corresponding initial shrinking velocity at the outer boundary, the CS soliton first shrinks at the outer boundary with velocity u_{im} to the inner boundary where it gets an effective energy input ΔE_i^{eff}, and then expands to the outer boundary with final velocity u_{fm} where it will get an effective energy change ΔE_e^{eff}, and then repeats this motion. It follows that

$$E_{im} + \Delta E_{oi} + \Delta E_i^{\text{eff}} + \Delta E_{io} = E_{fm} \tag{17}$$

where E_{im} and E_{fm} are the corresponding energy with respect to the velocity u_{im} and u_{fm}, respectively, [see Eq. (9)], and ΔE_{oi} and ΔE_{io} are the energy changes during the shrinking and expanding processes, respectively. The total energy change ΔE due to dissipation (the dissipation due to reflection has been taken into account in the effective energy inputs ΔE_i^{eff} and ΔE_o^{eff}) during a period is $\Delta E = \Delta E_{oi} + \Delta E_{io}$, combining Eq. (17) it becomes

$$\Delta E = E_{fm} - E_{im} - \Delta E_i^{\text{eff}} \ . \tag{18}$$

For a stable motion, this energy change is balanced by the net energy input $\Delta E_i^{\text{eff}} + \Delta E_o^{\text{eff}}$, or

$$\Delta E_i^{\text{eff}} + \Delta E_o^{\text{eff}} + \Delta E = 0 \ , \tag{19}$$

which is related to the minimum feeding current $\eta_{\min}$. It follows after some algebraic manipulation that

$$\eta_{\min} = \frac{2}{\pi} \left[\frac{1}{(1-u_{im}^2)^{1/2}} - \frac{1}{(1-u_{fm}^2)^{1/2}} \right] - \kappa_o + \pi\alpha \ . \tag{20}$$

The lower limit of the EBC is $\eta_{\min} + \kappa_o$ where κ_o is related to κ_i and ρ_i for junctions of width W. We have calculated the EBC limit following this treatment. Figure 4 shows the lower limit of the EBC versus ρ_i for $W = 7.5$, $\alpha = 0.06$, and different κ_i. Qualitative agreement with the simulation results is achieved for the negative applied field $\kappa_i = -0.56$. Note that a sudden change of the slope for the line with $\kappa_i = -0.56$ also exists like the one in Fig.

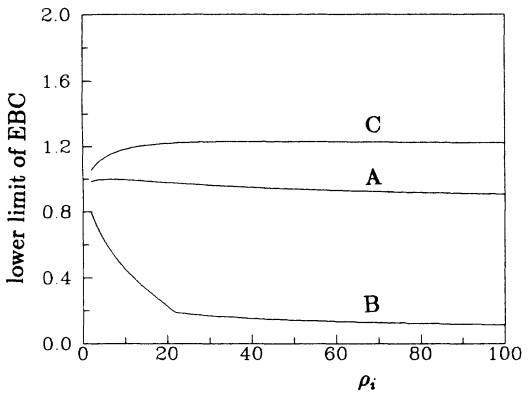

FIG. 4. The calculated ρ_i dependence of the lower limit of the EBC from the analytical treatment for $W=7.5$ and $\alpha=0.06$. Line A: $\kappa_i=0$; Line B: $\kappa_i=-0.56$; Line C: $\kappa_i=0.2$. Dimensionless quantities are used.

3(b), and we find that the slope change is due to the following fact. For small ρ_i, u_{fm} is zero, while for larger ρ_i, the "attraction" effect is minor, and the energy input $\Delta E_i(>0)$ at the inner boundary for $\kappa_i=-0.56$ is relatively so large that the CS soliton can be launched to the outer boundary with a final velocity u_f, and $u_f \geq u_{fm} > 0$. However, the analytically calculated results seem to have been over estimated compared with the simulated results for $\kappa_i=0$ and $\kappa_i=0.2$, and this is due to the over estimation of the reflection dissipation. The reflection dissipation appearing in Eq. (15) acts as an effective additional applied field with an amplitude of $\pi\alpha \approx 0.19$ ($\alpha=0.06$), which plays an essential role for $\kappa_i \geq 0$, since the CS soliton loses much energy at the inner boundary in this situation. However, in real CS soliton motion, the boundary reflection is not a sudden process as we have taken it in our analysis, and the reflection dissipation is velocity dependent.[35,36] Nevertheless, a qualitative conclusion can be drawn from Fig. 4 that, the lower limit of the EBC for negative applied field is significantly smaller than for a non-negative applied field, and therefore a negative applied field is expected to be favorable to CS soliton motion, so long as $|\kappa_i|$ is not too large.

It should be pointed out that in Fig. 3(a), if $\eta < \eta_{\min}$ the initial CS soliton state switches definitely to a zero voltage state because of the soliton return effect and the dissipation (or equivalently breather decay, the breather being the bound pair of returning soliton and the virtual antisoliton and vice versa), while if $\eta > \eta_{\max}$ the CS soliton state switches back to zero voltage state for smaller ρ_i (<10), and switches to rotational state for larger ρ_i (>15). This is quite natural, since both lines A and B end at $\rho_i=\rho_{\min}$; therefore the state switches similarly along both lines where the $1/\rho$ term in eq (1) plays an important role, while for larger ρ_i, the $1/\rho$ term has a minor effect and the state switching should be similar to that of a 1D in-line junction. For moderate ρ_i, the state switches at the upper limit rather undefinitely. We find that for junctions with smaller ρ_i, although a current step exists, the I-V curve shows a negative differential resistance $dV/d\eta$ before the switching to zero voltage state, and this might suggest a competition among various nonlinear modes. A similar phenomenon exists for the case of a negative applied field. In the above analysis, we have concentrated on state switching; other relevant studies have been made for the 1D overlap or overlap-like junctions, cf. Refs. 26, 27, and 32–34. The understanding of the state switching at the upper end of the current step is essential for the determination of the maximum height of the current step. As is well understood, the boundary conditions plays a major role in the process of state switching. The boundary conditions are equivalent to the existence of static virtual fluxons (or antifluxons) outside the ends of the junction (if $|\phi_\rho|<2$ there). However, as soon as the energy requirement for the creation of a fluxon into the junction is satisfied, a virtual fluxon will enter the junction and move in the direction such that its motion is aided by the bias current. In other words, an initially stable soliton is unlikely to remain so, i.e., state switching is likely to occur. We note that for the overlap junctions, the simplest power-balance perturbative scheme predicts an infinite current-step height,[37–39] while the perturbative scheme proposed in Refs. 26 and 27 predicts a maximum normalized step height equal to one (or $|\phi_x|=1$ at the boundary for the upper end of the 1-ZFS). In contrast, experimental and numerical results by various authors (cf. Ref 28) typically give a maximum step height between 0.4 and 0.8. In a further study Pagano *et al.* made a boundary-model analysis[29] and considered the behavior of the switching current of ZFS (less than one) with respect to junction length and dissipation. In our situation, the comprehensive mechanism that leads to the different state switching in our system deserves further investigation because of the in-line-like geometry and the appearance of the additional effect of the $1/\rho$ term that is responsible for the size effect.

In conclusion, the size effect in an annular junction is due to the ever increasing of the lower limit of the EBC (resulting from the minimum feeding current) and the decreasing of the upper limit of the EBC (relating the instability of the CS soliton state under high bias) with decreasing inner radius ρ_i.

We have further investigated other junctions with $W=5$ and $W=10$ and both with $\alpha=0.06$. For zero applied field, $\rho_{\min}=7.3$ for $W=5$ and $\rho_{\min}=20$ for $W=10$. For $\kappa_i=-0.4$, $\rho_{\min}=4.3$ for $W=5$. For $\kappa_i=-0.5$, $\rho_{\min}=2.7$ for $W=10$. We have confirmed, with these results, that the size effect exists and a negative applied field plays an important role in reducing the size effect, and this is of much interest in physical experiment and application for the preparation of an annular Josephson junction.

III. SUMMARY

In this paper, we have addressed the problem of the size effect in circularly symmetric, annular Josephson junctions by use of a full numerical simulation. There exists a minimum inner radius $\rho_{\min}$ for the annular junctions with dissipation α and width W and under an applied field. A negative applied field enhances the stability of CS soliton motion and makes it possible for a CS soliton to propagate in a junction with relatively smaller

inner radius, and vice versa. The role of the applied magnetic field is emphasized. We suggest that the size effect arises because for junctions with small ρ_i, the minimum feeding current is so large (due to soliton return effect and other factors) that the resulting boundary condition is unfavorable for the stability of CS soliton motion. The current range in the current step vanishes as $\rho_i \rightarrow \rho_{\min}$. State switching at the upper end of the current step, which is very involved for various values of ρ_i, deserves further consideration. The size effect, besides the soliton return effect, is typical in junctions with circular symmetry.

ACKNOWLEDGMENTS

We would like to acknowledge the support of the Chinese Natural Science Foundation for this work. We also thank Professor Kunming Xu for his helpful private communications.

[1]J. K. Perring and T. H. R. Skyrme, Nucl. Phys. **31**, 550 (1962).
[2]A. C. Scott, Am. J. Phys. **37** 1969.
[3]B. D. Josephson, Adv. Phys. **14**, 419 (1965).
[4]J. A. Krumhansl and J. R. Schrieffer, Phys. Rev. B **11**, 3535 (1975).
[5]T. R. Koehler, A. R. Bishop, J. A. Krumhansl, and J. R. Schrieffer, Solid. State Commun. **15**, 1515 (1975).
[6]M. J. Rice, A. R. Bishop, J. A. Krumhansl, and J. R. Schrieffer, Phys. Rev. Lett. **36**, 432 (1976).
[7]U. Enz., Hel. Phys. Acta **37**, 245 (1964).
[8]M. J. Ablowitz, D. J. Kaup, A. C. Newell, and H. Segur, Phys. Rev. Lett. **30**, 1262 (1973).
[9]A. Barone and G. Pagano, *Physics and Applications of the Josephson Effect* (Wiley, New York, 1982).
[10]M. B. Fogel, S. E. Trullinger, A. R. Bishop, and J. A. Krumhansl, Phys. Rev. Lett. **36**, 1411 (1976).
[11]J. F. Currie, S. E. Trullinger, A. R. Bishop, and J. A. Krumhansl, Phys. Rev. B **15**, 5567, (1977).
[12]D. J. Kaup and A. C. Newell, Proc. R. Soc. London Ser. A **361**, 413 (1978).
[13]K. H. Spatschek, Z. Phys. B **32**, 425 (1979).
[14]D. W. McLaughlin and A. C. Scott, Phys. Rev. A **18**, 1652 (1978).
[15]O. A. Lerving, N. F. Pedersen, and M. R. Samuelsen, J. Appl. Phys. **54**, 987 (1983).
[16]W. Wang and X. X. Yao, J. Phys. A **22**, 2447 (1989).
[17]W. Wang, A. L. Thomson, and X. X. Yao, Phys. Rev. B **43**, 2756 (1991).
[18]Q. H. Wang, W. Wang, and X. X. Yao, J. Appl. Phys. **71**(2), 1014 (1992).
[19]Q. H. Wang, W. Wang, and X. X. Yao, Phys. Rev. B **45**, 3013 (1992).
[20]W. Wang, Q. H. Wang, and X. X. Yao, J. Appl. Phys. **70**, 6970 (1991).
[21]Q. H. Wang, W. Wang, and X. X. Yao, J. Phys. C **4**, 4653 (1992).
[22]P. L. Christiansen and O. H. Olsen, Phys. Scr. **20**, 531 (1979).
[23]P. L. Christiansen and O. H. Olsen, Phys. Lett. A **68**, 185 (1978).
[24]I. L. Bogolubsky, Phys. Lett. A **61**, 205 (1977).
[25]J. Geike, Phys. Lett. A **98**, 147 (1983).
[26]S. Pagano, N. F. Pedersen, S. Sakai, and A. Davidson, IEEE Trans. Magn. MAG. **23**, 1114 (1987).
[27]A. Ferrigno and S. Pace, Phys. Lett. A **112**, 77 (1985).
[28]A. Davidson, B. Dueholm, B. Kryger, and N. F. Pedersen, Phys. Rev. Lett. **55**, 2059 (1985).
[29]S. Pagano, M. P. Soerensen, P. L. Christiansen, and R. D. Parmentier, Phys. Rev. B **38**, 4677 (1988).
[30]Y. M. Zhang and P. H. Wu (unpublished).
[31]I. L. Bogolubsky and V. G. Makhankov, Pis'ma Zh. Eksp. Teor. Fiz. **24**, 15 (1976); **25**, 120 (1977).
[32]B. A. Malomed, Phys. Rev. B **43**, No. 13 10 197 (1991).
[33]S. Pagano, M. P. Soerensen, R. D. Parmentier, P. L. Christiansen, O. Skovgaard, J. Mygind, N. F. Pedersen, and M. R. Samuelsen, Phys. Rev. B **33**, 174 (1986).
[34]S. E. Burkov and A. E. Lifshitze, Phys. Lett. A **16**, 71 (1984).
[35]Legrand, Phys. Rev. A **15**, 5068 (1987).
[36]N. F. Pedersen, M. R. Samuelsen, and D. Welner, Phys. Rev. B **30**, 4057 (1984).
[37]J. M. Salerno, M. R. Samuelsen, G. Filatralla, S. Pagano, and R. D. Parmentier, Phys. Lett. A **137**, 75 (1989).
[38]J. M. Salerno, Phys. Lett. A **144**, 453 (1990).
[39]O. H. Olsen, N. F. Pedersen, M. R. Samuelsen, H. Svensmark, and D. Welner, Phys. Rev. B **33**, 168 (1986).